applied sciences

MDPI

Article

A Hybrid Deep Learning Framework Based on Diffusion Model and Deep Residual Neural Network for Defect Detection in Composite Plates

Tianrui Huang, Yang Gao *, Zhenglin Li, Yue Hu * and Fuzhen Xuan

Shanghai Key Laboratory of Intelligent Sensing and Detection Technology, School of Mechanical and Power Engineering, East China University of Science and Technology, Shanghai 200237, China
* Correspondence: yanggao@ecust.edu.cn (Y.G.); huyue1990@ecust.edu.cn (Y.H.)

Abstract: The establishment of a structural health monitoring (SHM) system for the damage and defects of composite structures is of great theoretical and engineering value to ensure their production and operational safety. Advanced machine learning technologies, such as deep learning, have become one of the main driving forces for state monitoring and predictive analysis of these structures. However, it is difficult to obtain sufficient data to train the deep learning model, which may fail to build an accurate and efficient SHM model. To overcome this problem, a new method based on Lamb waves and the diffusion model (DM) is proposed to realize the identification and classification of different defects for carbon-fiber-reinforced polymer (CFRP) structures. In this study, DM is used as the generation model of data enhancement, and the optimized and improved DDPM model is constructed in this experiment. The deep residual neural network (DenseNet) is used to identify and classify the defect features from the Lamb wave signals. Experimental and test results show that the deep learning framework designed in this study based on DenseNet classification and DDPM data enhancement can accurately detect and classify damage signals of common defects in CFRP composite plates.

Keywords: structural health monitoring; diffusion model; DenseNet; Lamb wave

Citation: Huang, T.; Gao, Y.; Li, Z.; Hu, Y.; Xuan, F. A Hybrid Deep Learning Framework Based on Diffusion Model and Deep Residual Neural Network for Defect Detection in Composite Plates. *Appl. Sci.* **2023**, *13*, 5843. https://doi.org/10.3390/app13105843

Academic Editor: Claudio Guarnaccia

Received: 18 February 2023
Revised: 25 March 2023
Accepted: 25 March 2023
Published: 9 May 2023

1. Introduction

Carbon-fiber-reinforced polymer (CFRP) has high strength-to-weight ratio, high stiffness-to-weight ratio, light-weight, corrosion resistance, fatigue resistance, designability and other properties, and is widely used in aerospace, energy buildings, sports equipment, land transportation, marine fields, etc. In the context of the depletion of mineral energy, the global natural gas trade is active, and the market is increasing. Accordingly, composite wound gas cylinders commonly used for hydrogen storage or energy storage are also being used more widely and have a better prospect [1,2].

The appearance of commonly used composite gas cylinders is shown in Figure 1. However, improper storage, prepreg production and preparation of CFRP during material processing may lead to fiber fracture, matrix debonding, fiber migration and other damages. During component manufacturing, fiber delamination, kinking, blistering, pollution, holes and other damages are caused due to improper laying, curing, machining or assembly. In service engineering, fiber delamination, fracture, erosion, matrix cracking and other damages may be caused by collision, chemical corrosion, local overload, fatigue and harsh environments. Due to the accumulation of impact, load, service time, environment and other factors, fatigue damage is the most dangerous and the main form of mechanical structure failure in the service process, accounting for 50–90% of the total mechanical structure failure [3]. At the initial stage, there will be slight fatigue damage in the structure, which is difficult to detect. The internal fatigue damage gradually expands, and when it expands to a certain extent, it will break, and when it is serious, it will cause huge economic

losses and endanger personal safety [4]. Because of this, composite gas cylinders also have high safety risks, and now many accidents caused by the health problems of gas cylinders have aroused everyone's attention. Therefore, it is of great significance to monitor and evaluate the health status of CFRP in real time, and efficient detection and monitoring technology has become the focus of current research. Currently, many people are studying experiments on composite plates and cylinders. Generally, basic research can be carried out on plates before being extended to gas cylinders.

Figure 1. Hydrogen storage composite wound cylinder.

At present, major research institutions have developed many structural health monitoring (SHM) methods. Common SHM methods include the acoustic emission method, electromechanical impedance method, vibration method, strain method, Lamb wave method, etc. Among them, the acoustic emission method depends on the acoustic emission signal when the damage occurs and expands, which is suitable for online use; The electromechanical impedance method is low in cost and simple in structure, but it is difficult to detect minor damage with low accuracy and small monitoring range [5,6]. Although the vibration method can monitor large-area damage, it requires more sensors, is insensitive to small damage, and is easily affected by the external environment; The strain method is only applicable to the monitoring of large-scale damage to structures. Compared with other SHM methods, because Lamb wave propagates in the measured structure with small signal attenuation, long propagation distance, sensitivity to minor damage, large area monitoring, high accuracy, low cost and other advantages, the structural health monitoring method based on Lamb wave is widely used in the industrial field and favored by researchers at home and abroad [4].

Piezoelectric (PZT) is the main sensing element used in Lamb wave experiments at present and is widely used in signal generation and the acquisition of Lamb waves. A piezoelectric ceramic chip is a dual-mode transducer made of zirconium, titanium and lead oxides after chemical reaction. The structure includes a piezoelectric ceramic sheet and metal vibration sheet, which have obvious piezoelectric characteristics and can be used for ultrasonic excitation and reception.

Our current research mainly focuses on the corresponding signal acquisition and subsequent identification processing for several types of common CFRP damage, such as holes, notches, fatigue cracks, etc. This study is based on the health monitoring principle of Lamb wave. A Lamb wave in composite laminate is an elastic wave generated and propagated between the upper and lower surface boundaries of the plate by particle movement, as shown in Figure 2. When the wave packet encounters a defect, reflection and scattering occur. Then, by analyzing the difference in waveform signals between healthy samples and damaged samples, the defects in the medium can be easily detected.

Compared with broadband excitation signal, narrowband excitation signal is more suitable for structural health monitoring technology [7]. The active Lamb wave is excited by the driving element to the monitored structure. Lamb wave has been widely used in the detection of materials and plates due to its flexible excitation and detection methods, its interaction with plate defects and carrying a large amount of information required for detection. Additionally, it has become an important and effective means and method for evaluating the performance of plate-like structures. In 2011, Mirahmadi et al. [8] effectively improved the time resolution and signal-to-noise ratio of Lamb wave S0 mode detection by using signal processing methods such as Wiener filtering. In 2021, Xiang Yanxun from East China University of Science and Technology proposed a crack localization method based on group velocity matching, which can well locate breathing cracks on the guided wave propagation path [9].

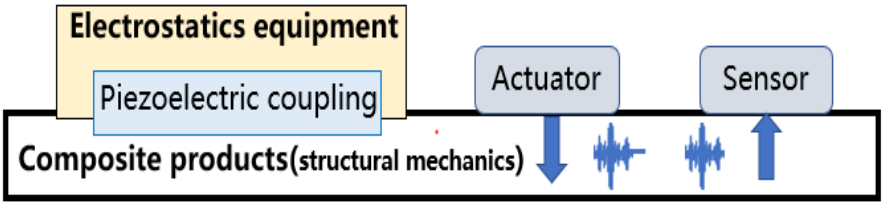

Figure 2. Schematic diagram of ultrasonic signal excitation propagation and reception.

Recently, intelligent manufacturing has been thriving, and various types of production data can be collected faster and more extensively than ever before. This provides new opportunities for data-driven fault diagnosis methods to fully utilize massive data of various types [10], which has attracted increasing attention from researchers and engineers. In the rapidly developing world of technology, artificial neural networks are one of the most mature data-driven fault diagnosis methods. With the rapid development of machine learning, deep learning (DL) has become an effective method for structural health monitoring. DL can automatically learn abstract representations of raw data [11], which can better extract features and improve analysis effectiveness. In certain scenarios, data types for fault diagnosis can be presented in two-dimensional formats (such as time-frequency spectra), and then combined with image processing methods for classification. Through the processing of these images, analysis of various time-series signals can be facilitated, providing better ideas and directions for structural health monitoring today [12]. Ince et al. [13] applied one-dimensional CNN to real-time motor fault diagnosis in their research. Abdeljaber et al. [14] conducted experiments on real-time damage detection using one-dimensional CNN. Chong [15] proposed a method for extracting induction motor fault features, in which he converted one-dimensional vibration signals into two-dimensional grayscale images. Liu et al. [16] applied a CNN model to wave-based crack damage detection, training a deep CNN model based on Lamb waves data to avoid the calculation and extraction of damage features. Wu et al. [17] used continuous wavelet transform to convert Lamb wave time series signals into two-dimensional images, and then used a CNN model to classify the images, achieving accurate localization of layered damage in composite structures. Through these methods, researchers can simplify the process of waveguide signal processing, and to a certain extent, simplify the analysis of waveguide's multimode and dispersion problems, while also improving the ability to extract signal features. At the same time, these methods can be combined with image processing methods for signal classification, improving the classification effect of temporal signals. However, in practice, damaged and defective data is relatively rare and costly. There are also many challenges in the engineering application of this technology, including the lack of training data, the imbalance between damaged and undamaged data, and the impact on the construction and subsequent processing of the overall dataset. Therefore, in this study, we hope to find a method to expand the acquired damaged signal samples without affecting accuracy, and improve this situation through data augmentation, combined with innovative classifiers

to optimize signal classification. In the signal dimension transformation method, commonly used methods have many limitations and complex parameters, and the effect of feature extraction for Lamb waves is generally not ideal. Therefore, this study attempts a new signal-to-image conversion method, which can extract Lamb wave features more specifically, simplify the processing process, and improve the effect of signal dimension transformation. In addition, this study uses attention mechanisms to capture the time and feature dependencies of time series, improving the quality of data generation and subsequent signal classification. This overall framework for deep learning and signal processing is the focus of this study

The rest of this article is organized as follows. Section 2 is about the design of the experimental scheme and the introduction of relevant experimental equipment and materials. Section 3 includes the selection and design of data enhancement algorithm and signal classification algorithm. Section 4 presents the experimental test results of the proposed method and the comparison of common methods. Finally, Section 5 concludes this article.

2. Description of the Experiment

2.1. Experimental Object and Characteristics

Considering that it is difficult to carry out experiments on the surface of a cylinder, this study firstly simplifies the experimental object to a plate for simulation and testing. Through the preliminary design and improvement of the distributed network array on the plate, the subsequent signal acquisition and analysis experiments are carried out. After the experimental results of the plate are obtained, the experiment will be extended to curved surfaces and cylinders. The plate and corresponding sensors used in the experiment are shown in Figure 3.

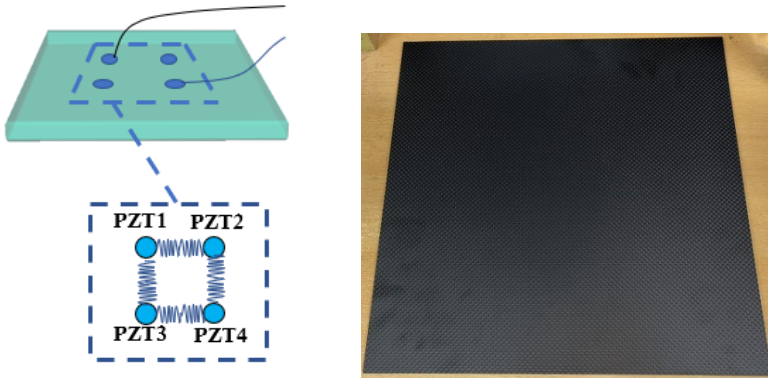

Figure 3. Photos of the composite material plate and layout diagram of sensors.

In this experiment, carbon fiber/epoxy resin matrix composites are used. The test structure is given by carbon-fiber-reinforced polymer (CFRP) plates with clearly defined geometry and piezoelectric transducers. Composite laminates are generally composed of many basic sub layers laid in different directions and superimposed. The adjacent sub layers of laminates are usually bonded by a thin adhesive layer. The composite winding layer can bear most of the pressure load, in which the fiber is the main carrier. The resin plays a bonding role on the fiber, and it also plays a role in distributing and transferring the load between the fibers. Therefore, we need to select high-strength and high-elasticity reinforcing fiber and resin with excellent performance to improve the bearing capacity of the structure. The details of the raw materials of the composite plate used in this experiment are as follows. The reinforcing material is T700SC12K carbon fiber from Toray Corporation of Japan. The matrix material is epoxy resin and imidazole curing agent, whereas the main component of epoxy resin is bisphenol A epoxy resin. Three CFRP plates were manufactured for this study with the dimensions of 300 mm × 300 mm and a thickness of 4.8 mm, and the paving method is $[+45^\circ/0^\circ/-45^\circ/90^\circ]_{6s}$. According to the above stacking method, different perspectives are used for stacking, and the thickness of a single layer

board is about 0.2 mm. A total of 24 layers are laid in the whole. The first specimen, called "Intact plate", was used for acoustic field measurement and related parameter measurement under the condition of structural integrity. The second sample, called "Hole plate", was used to obtain the Lamb wave data in the case of hole defects in the plate. The third sample, called "Crack plate", was used to obtain the Lamb wave data in the case of crack defects in the plate. The elastic modulus and shear modulus of composite materials are anisotropic, so 9 elastic constants are needed to describe their mechanical behavior. These 9 elastic constants can be divided into 3 principal directions of elastic modulus (E), 3 principal directions of Poisson's ratio (ν), and 3 principal directions of shear modulus (G). These 9 quantities constitute the main mechanical performance parameters of composite material plates in experiments. The mechanical property parameters of carbon fiber/epoxy resin matrix composite single-layer plate are shown in Table 1.

Table 1. Materials' parameters of carbon fiber/epoxy composites.

E_{11}/MPa	E_{22}/MPa	E_{33}/MPa	ν_{12}	ν_{13}	ν_{23}	G_{12}/MPa	G_{12}/MPa	G_{13}/MPa
172,000	7000	7000	0.35	0.35	0.35	3900	3900	3900

2.2. Experimental Equipment and Principle

The active Lamb wave is excited by the driving element to the monitored structure. The active Lamb wave is received by the receiving sensor after propagating a certain distance in the structure. Then the Lamb wave signal containing damage information is processed by using a specific signal processing method, and the characteristic parameters related to the monitored structure damage are extracted, and the structural damage is identified by combining the corresponding damage identification methods. The ultrasonic excitation system of this experiment is the RETIC RAM SNAP 5000 high-energy ultrasonic measurement system. The RETIC RAM SNAP 5000 high-energy ultrasonic measurement system is used for the excitation and measurement of ultrasonic Lamb waves. This measurement system was specially developed by the RITEC Corporation of the United States for the measurement of nonlinear ultrasound. It is a commercial nonlinear ultrasonic measurement system with advanced technology at present. It mainly includes a broadband RF pulse amplifier, signal tracking receiver, phase shift sensitive detector, gate integrator and multiple frequency synthesizers. The ultrasonic measurement system generates pulse signals according to the indication information, which are transmitted to the ultrasonic piezoelectric transducer through the attenuator and low-pass filter through the connecting line. The transducer converts ultrasound signals into vibration signals through the reverse piezoelectric effect, and injects them into the plate through the piezoelectric element, so that they propagate into the plate. The excited Lamb wave propagates in the sheet and interacts strongly with the sheet defect. The signal with a large amount of information required for detection enters the receiving transducer, and is displayed and stored by the oscilloscope after passing through the high-pass filter and amplifier. The received signal is processed to obtain the desired information. The specific experimental equipment diagram and recommended schematic diagram are shown in Figure 4.

The RETIC RAM SNAP 5000 high-energy ultrasonic measurement system generates 5-cycle Hanning window modulated sine pulse signals, drives ultrasonic piezoelectric transducers to generate ultrasonic vibration signals after passing through attenuators, and applies these vibration signals to sample objects for experiments. A signal with 5 cycles ensures that the waveform in the time domain is easy to distinguish while maintaining a narrow bandwidth. The Hanning window modulation used in our experiment can increase the main lobe, reduce the side lobes, and reduce spectral energy leakage. The Lamb wave is generated in the flat sample and propagated to the receiving piezoelectric transducer. Then the signal is amplified by the power high voltage amplifier, and then the signal is converted from an electrical signal to a mechanical signal through the PZT driver and propagated in the plate structure. Then it is received by the PZT sensor and converted into electrical

signal again. Finally, the received signal is input into the RETIC RAM SNAP 5000 system, oscilloscope and computer for storage, display, and subsequent processing and analysis.

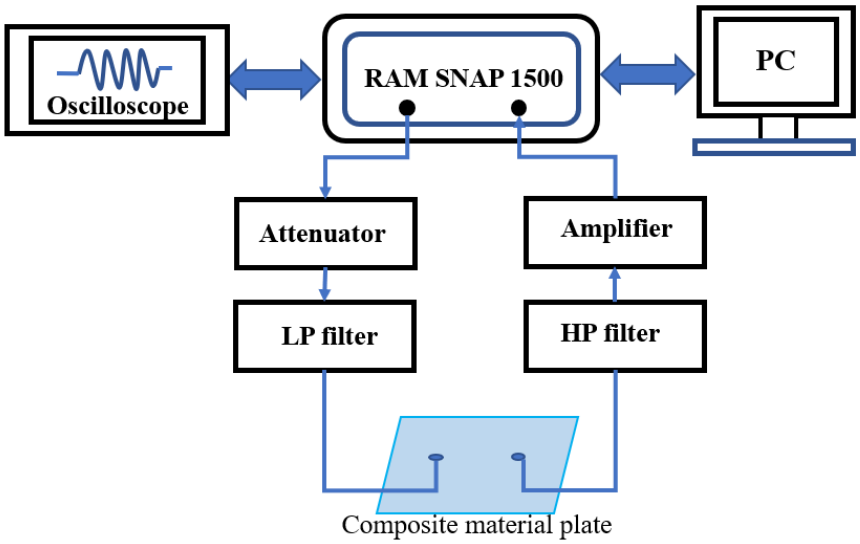

Figure 4. Ultrasonic excitation system equipment and experimental principle.

For this experimental design, Lamb wave is selected as the detection method. The wave velocity of the same guided wave mode will change with the change in frequency. At the same time, the increase in frequency will also lead to more complex guided wave modes. Not only do the modes increase, but also different modes with wave velocity close to will mix and interfere, increasing the difficulty of signal processing and affecting the detection accuracy. Here, the phase velocity of the fundamental symmetric (S0) Lamb wave mode was used to establish the model for evaluating the extent of the damage. In this research, the center frequency of 210 kHz is selected as the excitation frequency after the verification of experiment and simulation. At this frequency, the guided wave mode is the least, and the wave velocity does not change significantly with the frequency, which is conducive to modal separation. At the same time, selecting a lower frequency can reduce the attenuation of signal transmission, which is suitable for the monitoring of relatively large composite structures.

2.3. Experiment Design and Preparation

Defect pre-setting is shown in Figure 5. The defects are set in the middle of the laminate, mainly including hole defects and crack defects. In this experiment, both hole defects and crack defects are preset in the center of the plate. The diameter of the hole is set to be 5 mm, with a depth of 3 mm. The size of the crack is approximately 1.5 mm × 30 mm, with a depth of 1 mm. According to the previous statement, this experiment selects a center frequency of 210 kHz as the excitation frequency. Correspondingly, the sampling frequency for the time sequence signal in this experiment is chosen as 9×10^6 Hz, and the amplitude of the excitation signal is set to 1 mV. In this experiment, the excitation frequency of the guided wave signal is 210 kHz, and the longest time for the propagation of the guided wave direct wave signal in the structure is calculated to be 0.000058 s, based on the wave speed of the corresponding guided wave slowest mode at this frequency. Therefore, to ensure the complete acquisition of the guided wave signal, a storage time length of 0.0001 s, which is greater than this value, is selected for the signal automatic acquisition system. As the selected sampling point count is set to 5×10^6 per second, 500 data points can be collected for each sensor path. This is then used as the window length for extracting a set of signal data. Each signal was taken as a whole set of data for subsequent training without being cut or segmented. The PZT sensor array is arranged symmetrically in the center, forming a square shape. The piezoelectric disk measures 8 mm in diameter. PZT sensors are arranged at four ends as excitation and reception sources.

All PZTs can be used as actuators and sensors in the experimental testing process. The PZTs are bonded to the surface of the composite plate using cyanoacrylate adhesive. Compared with other adhesives, this adhesive is more suitable for quickly bonding PZT sensors in short-term experiments. When pasting the sensors, keep the bonding surface clean and flat. As shown in the schematic diagram in the article, we sequentially numbered the PZT sensors as PZT1, PZT2, PZT3, and PZT4, and stimulated the excitation signal from PZT1 to PZT4 in turn. When each sensor is stimulated, the other three sensors receive the signal. Therefore, we can obtain 12 sets (4×3) of Lamb wave signals in one monitoring experiment. First, ultrasonic nondestructive testing is conducted on the specimens to verify their intact state and obtain the signal data in the intact state. Multiple groups of one-dimensional time series signals under different defects are obtained by repeated experimental tests. By repeating the test in this way, multiple sets of signal data can be obtained, and the current data set constructed is 360 sets of signal data. These data constitute a large enough data set, which can reflect the main characteristics of this defect. This data set can be used for subsequent experiments and algorithm analysis to extract the features and signal information of corresponding defects.

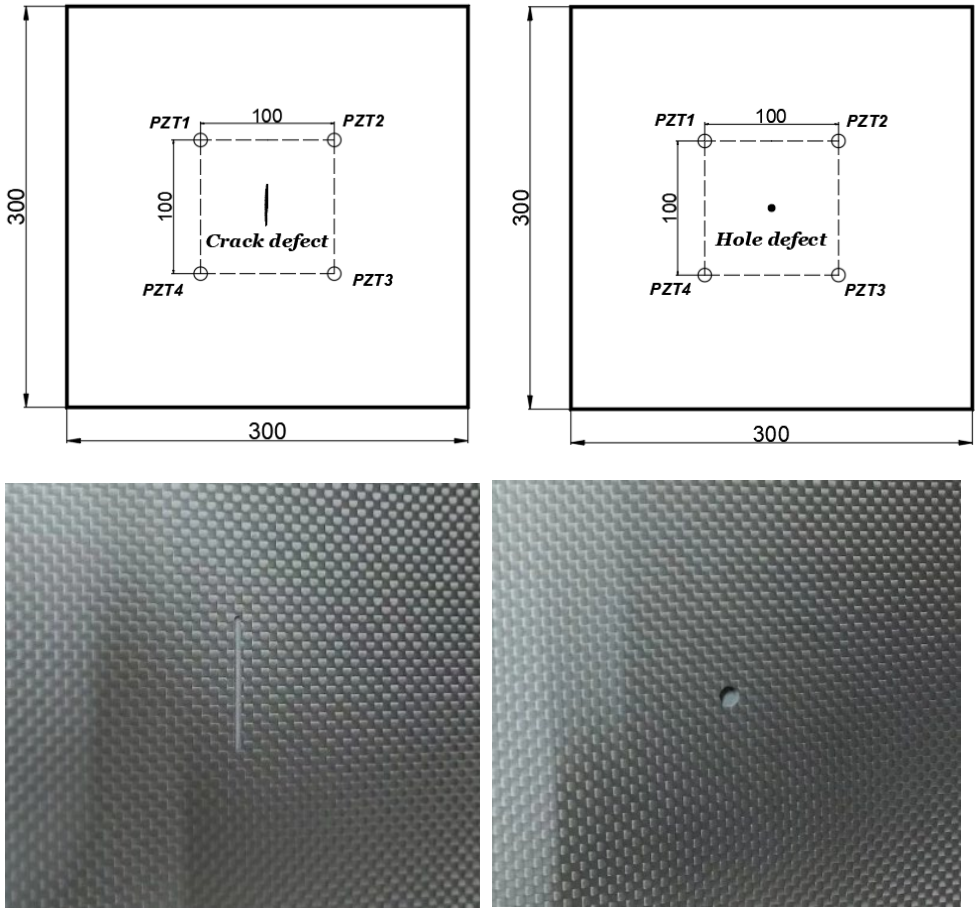

Figure 5. Default defect diagram and actual defect diagram (unit: mm).

3. Methodology

In order to realize the identification and classification of different damages and defects, neural networks are considered for processing. Processing direction mainly faces the application of data-driven modeling within the concepts of sensor data fusion, feature extraction and pattern recognition for Lamb wave signals. Data-driven methods require a large volume of historic data to establish the fault modes of the systems without a priori known models or signal patterns. The ultrasonic Lamb wave signal is obtained during the experiment, and the neural network model is constructed and trained using the signal data obtained from the original sample. The neural network model automatically learns the

mode and damage-sensitive characteristics of ultrasonic signals during training. It should be added that in practice, data in damaged cases are rare and very costly. There are also many challenges in the engineering application of this technology, including the lack of training data, the imbalance between damaged and undamaged data, and the impact on the construction and subsequent processing of the overall dataset. Therefore, it is necessary to find a method to expand the obtained damage signal samples without affecting the accuracy. The underlying neural networks are trained on a small subset of data and are then used to process any incoming new sample. Considering these premises and foundations, the target model is selected and parameterized. On the basis of parametric research, the structure and parameters of the model are optimized. The test signal is introduced into the optimized model to verify the damage detection capability and classify the defects and damages. The idea in this study is to design a composite framework for identifying and classifying complex damage signals based on data augmentation and signal classification. At the same time, a dimension transformation method is introduced to process time series signals, which converts one-dimensional time series signals into two-dimensional images, making it easier to combine data with the latest and most mature neural network systems. In the specific operation process, we continuously optimize and improve the model by adding attention mechanisms and designing other relevant parameters. The theoretical basis, method selection and design of this study are depicted in Figure 6:

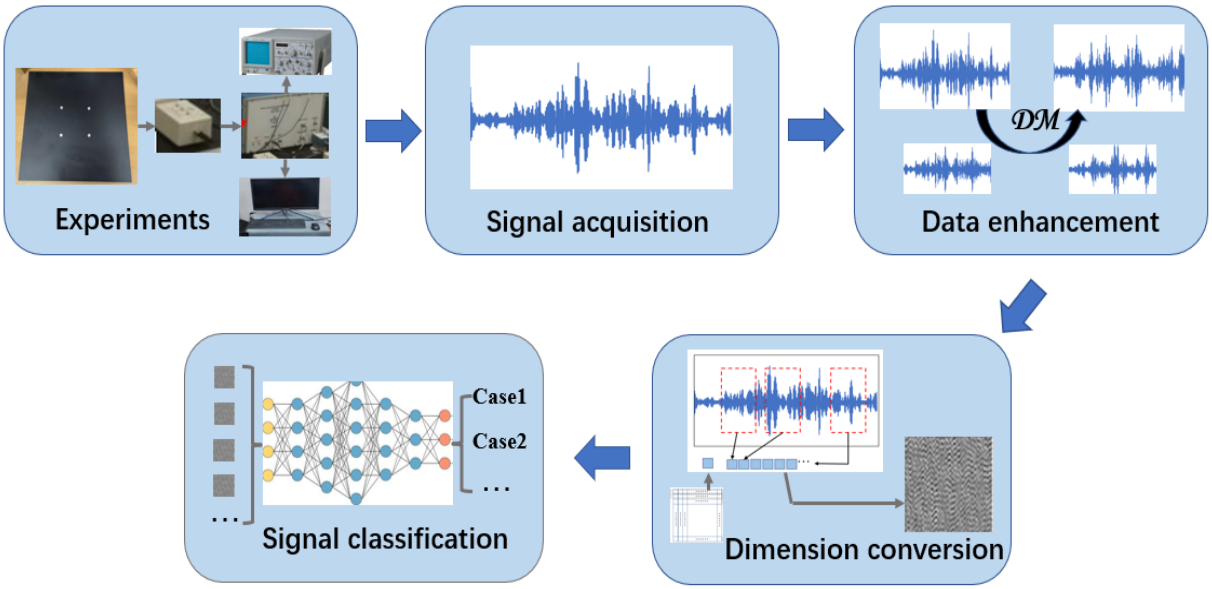

Figure 6. Flowchart of overall theory and experimental design.

3.1. A Method of Signal Dimension Conversion

In the acquisition experiment of Lamb waves, the collected signals are timing signals, which need to be processed and analyzed later. In traditional fault diagnosis methods, the data pre-processing method is vital since most data-driven methods cannot handle the raw signals directly. One of the main functions of the data pre-processing method is to extract the features of the raw signals from a large volume of historic data. However, extracting the proper features is exhaustive work, and these features have great effects on the final results. In addition, current deep learning methods mainly deal with two-dimensional structural data. The depth learning methods used for image processing are relatively mature, and there are many effective methods. Therefore, if we can convert the experimental one-dimensional time series data into two-dimensional (image) data through specific methods, we can better adapt to the current popular and cutting-edge models and improve the training and classification effect. Now, the following methods are adopted to convert the time-domain raw signals to images.

As shown in Figure 7, in this conversion method, the time-domain raw signals fulfill the pixels of the image by sequence. First, we need to obtain an $M \times M$-sized image. To fill the square image, we need to randomly intercept a segment signal with the length M^2 from the raw signal. First, let $L(i)$, $i = 1 \ldots M^2$ denote the value of the segment signal. While $P(j,k)$, $j = 1 \ldots M, i = 1 \ldots M$ denotes the pixel strength of the image, as shown in equation $P(j,k) = round\left\{\frac{L((j-1)\times \mathrm{M}+\mathrm{k})-Min(L)}{Max(L)-Min(L)} \times 255\right\}$ [18]. Later, we will analyze this formula. The value of the segmented signal at each position is defined by L , and the value corresponding to a specific position is determined by j and k. The image intensity at the corresponding position is obtained by performing the operation in the equation.

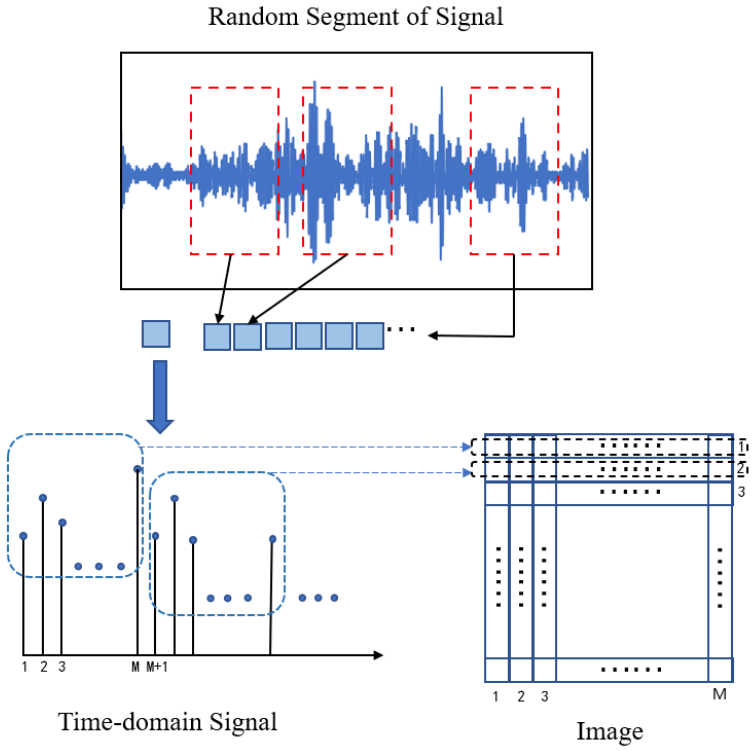

Figure 7. Schematic diagram of signal dimension conversion principle.

The function *round* is the rounding function, and the whole pixel value has been normalized from 0 to 255. The number size refers to the pixel intensity of the grayscale image. The 2 × 2 filters are commonly used in this study, and the size of image features on each layer would be reduced by half. Therefore, the recommended value of M in this case is 2^n. In this study, the selection of 64 × 64 and 16 × 16 depends on the amount of signal data. In combination with the sparsity of guided wave signal features and the large amount of data collected each time, in order to ensure the features of the data, 64 × 64 images are chosen as the research object. The advantage of this data processing method is that it can convert one-dimensional signals into two-dimensional signals through this method, and it provides a way to explore the 2D features of the raw signal [15]. Moreover, this data pre-processing method can be calculated without any predefined parameters and can reduce the experiences as more as possible. These can simplify the training process and optimize the calculation process. In this study, the size of the image varies with the volume of the signal data, and the guided wave signal data targeted in this experiment has a large volume. Moreover, a larger image size can facilitate classification results. Therefore, in this study, the size of the image is 64 × 64. In the subsequent processing, we also apply the zero-padding method to the model to prevent dimension loss. The process of quantifying temporal signals into two-dimensional images may introduce noise, which can cause the loss of image clarity and details, thereby affecting image performance to some extent. Therefore, this experiment used filters for the generated images, and in this experiment,

we chose the common Gaussian filter to smooth the image and remove noise. Through subsequent testing, this experiment minimized the impact of noise on image quality and subsequent processing as much as possible.

3.2. Data Enhancement Based on Diffusion Model

This study mainly aims to build a data-driven SHM system, which, most importantly, needs data support. Considering the limitations of the experimental conditions and the specific conditions of the experimental object, some experimental signals have poor detection effects, and some experiments have insufficient signal detection to build a sufficient number of data sets for training. It may have certain impact on the training of the experimental model, and will also have a certain interference with the analysis of the experiment. At the same time, the experimental data has uneven samples, so we consider expanding and enhancing some data to increase the number of samples. Data enhancement is also called data amplification, which means that limited data can generate the value equivalent to more data without substantially increasing data. These can expand the dataset, improve the robustness of the model, improve the generalization ability of the model and avoid sample imbalance. Now, we mainly consider testing several generation models in this study, including Generic Adversary Network (GAN), Variable Automatic Encoder (VAE) and diffusion models (DM).

3.2.1. GAN

GAN consists of a generator and discriminator. The generator is responsible for generating realistic data to "cheat" the discriminator, and the discriminator is responsible for judging whether a sample is real or "made". The training of GAN involves the two models learning from each other and obtaining new data through confrontation. The generating network should constantly optimize the data generated by itself so that the discriminant network cannot judge, and the discriminant network should also optimize itself to make its judgment more accurate. The relationship between the two forms confrontation, so it is called a confrontation network [19]. When selecting GAN, after comparison and analysis, the more advanced and practical DCGAN network was selected. DCGAN is a variant of GAN. DCGAN combines CNN with the original GAN, and both the generating network and the recognition network are applied to the deep convolution neural network. DCGAN improves the stability of basic GAN and the quality of generated results, and improves the ability and effect of feature extraction as a whole.

3.2.2. VAE

VAE wants to train a generation model. First, it assumes the distribution of a hidden variable z, and constructs a model $x = g(z)$ from z to target data x, which can map the sampling probability distribution to the training set probability distribution. The hidden variable z is generated, which contains data information and noise, so that the learned target data is close to the probability distribution of the real data. VAE generally matches a Gaussian distribution for each sample, and the hidden variable Z is obtained by sampling from the Gaussian distribution. In addition to restoring input sample data, it can also be used to generate new data. VAE is also a mature model for data generation and expansion.

3.2.3. Diffusion Model

A diffusion model is a kind of generation model, different from Variable Automatic Encoder (VAE), Generic Adversary Network (GAN) and other generation networks. A diffusion model gradually applies noise to the image in the forward phase until the image is damaged and becomes a complete Gaussian noise, and then learns the process of restoring from Gaussian noise to the original image in the reverse phase. The purpose of a diffusion model is to decompose specific data distribution $p(x)$ and reconstruct data step by step from random noise. Because the intermediate process is stochastic and unstable, the whole

process is generated. In addition, reversible random steps ensure extensive fidelity of the model and sample quality.

Specifically, in the forward phase, the noise is gradually increased on the original image, and the new image obtained in each step is only related to the results in the previous step until the image becomes pure Gaussian noise. The diffusion process is a Markov process. The reverse phase is a process of continuous noise removal. This is to give Gaussian noise to the original image, and then gradually remove the noise until the original image is finally restored [20]. The schematic diagram of the forward and reverse processes of the diffusion model is shown in Figure 8. More detailed processes will be described later:

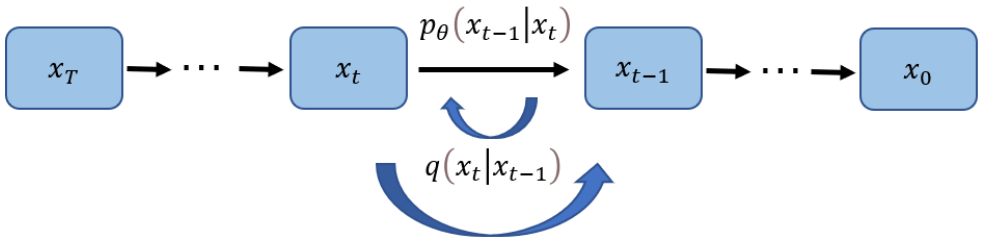

Figure 8. Schematic diagram of forward and reverse processes of the diffusion model.

These are the following points about the forward process. We have a sequence of T variables, where $x_0 \sim p(x)$ is our observed data and $x_{1:T}$ are latent variables. we can think of diffusion models as a specific realization of a hierarchical VAE. What sets them apart is a unique inference model, which contains no learnable parameters and is constructed so that the final latent distribution $q(x_T)$ converges to a standard gaussian [21]. This "forward process" model is defined as follows:

$$q(x_t|x_{t-1}) = N\left(x_T; x_{t-1}\sqrt{1-\beta_t}, \beta_t I\right) \tag{1}$$

The variables $\beta_1 \ldots \beta_T$ define a fixed variance schedule, chosen such that $q(x_T|x_0) \approx N(0, I)$. The forward process transforms sample distribution into gaussian noise. The image is transformed according to Gaussian distribution after adding noise. A nice property of the forward process is that we can directly sample from any timestep. Next, parameter transformation and iteration are carried out to obtain a new expression of the formula:

$$\alpha_t = 1 - \beta_t \tag{2}$$

$$\overline{\alpha_t} = \prod_{s=1}^{t} \alpha_s \tag{3}$$

$$q(x_T|x_0) = N\left(\sqrt{\overline{\alpha_t}}\, x_0, (1-\overline{\alpha_t})I\right) \tag{4}$$

One consequence of this is that we can draw random samples $t \sim \{1 \ldots T\}$ as part of the training procedure. Another consequence is that we can make additional manipulations to the lower bound to reduce the variance. This proceeds by observing the following result (from Bayes rule):

$$q(x_t|x_{t-1}) = \frac{q(x_{t-1}|x_t)q(x_t)}{q(x_{t-1})} \tag{5}$$

Due to the Markov property of the forward process, we have: $q(x_t|x_{t-1}) = q(x_t|x_{t-1}, x_0)$. Therefore, by conditioning all terms on x_0 we arrive at the following expression.

$$q(x_t|x_{t-1}) = \frac{q(x_{t-1}|x_t, x_0)q(x_t|x_0)}{q(x_{t-1}|x_0)} \tag{6}$$

This is the main framework of the forward process. Now, let us look at the reverse process.

The real noise generated by each forward propagation part is recorded as a label. In addition to inference, the forward diffusion process also includes the "data set construction process" similar to that used in this mathematical model. When the model is in reverse diffusion, the Gaussian noise generated in the forward diffusion can be predicted and inferred step by step to restore the initial sample data. The corresponding reverse process distributions are defined as:

$$p_\theta(x_{t-1}|x_t) = N\left(x_{t-1}; \mu_\theta(x_t, t), \sigma_t^2 I\right) \tag{7}$$

The variance σ_t^2 is a time-dependent constant (β_t). The $\mu_\theta(x_t, t)$ is a neural network with an input x_t. In order to share parameters between timesteps, the conditioning variable t is introduced in the form of positional embeddings [22]. The forward process samples x_t can be written as a function of x_0 and some noise $\epsilon \sim N(0, I)$.

We assume $p(x_{t-1}|x_t)$ is a Gaussian distribution, and we can use a neural network to fit it. Combine the generated noise tags as training reference. The inverse process is also a Markov chain process.

$$p_\theta(x_{0:T}) = p(x_T) \prod_{t=1}^{T} p_\theta(x_{t-1}|x_t) \tag{8}$$

The corresponding process and results can be obtained as $q(x_{t-1}|x_t, x_0)=\frac{q(x_t|x_{t-1},x_0)q(x_{t-1}|x_0)}{q(x_t|x_0)}$. Set variance to constant β_t, and continue to substitute the Gaussian probability density function for subsequent processing.

Finally, it can be summarized as such:

$$q(x_{t-1}|x_t, x_0)= N\left(x_{t-1}; \frac{(1-\overline{\alpha_{t-1}})\sqrt{\alpha_t}x_t}{1-\overline{\alpha_t}} + \frac{\beta_t\sqrt{\overline{\alpha_{t-1}}}x_0}{1-\overline{\alpha_t}}, \frac{1-\overline{\alpha_{t-1}}}{1-\overline{\alpha_t}}\beta_t\right) \tag{9}$$

Then, calculate the likelihood function of the target data distribution, so that the network can be trained. The mean fitted is $\mu_\theta(x_t, t) = \frac{1}{\sqrt{\alpha}}(x_t - \frac{\beta_t}{1-\overline{\alpha_t}}\epsilon_\theta(x_t, t))$, and this can be used for sampling.

The subsequent sampling process samples x_T from the standard normal distribution and calculates x_{t-1} iteratively. Known mean $\mu_\theta(x_t, t)$ and constant variance β_t, x_{t-1} to x_0 can be calculated by parameter renormalization. This training objective also be viewed as a weighted combination of denoising score matching used for training score-based generative models [23].

In fact, the idea of the Denoising Diffusion Probabilistic Model (DDPM) is very simple. In reverse diffusion, X_t is used to predict X_{t-1} images. Instead of optimizing the X_t to X_{t-1} conversion, it is to optimize how noise is added when X_{t-1} to X_t. At the same time, DDPM also adds time embedding [24]. In this model, we will use U-Net. U-Net is a U-shaped network structure, which is widely used in the segmentation field. The structure of this network is symmetrical, filled with convolutional layers but without fully connected layers. This method combines high-resolution feature maps with low-resolution feature maps after upsampling, which makes the segmentation results more accurate. At the same time, in the upsampling stage, the model still has a large number of channels, and more detailed object information will be transmitted back through upsampling. From the shape, the upsampling stage and the downsampling stage are symmetrical. The function of time embedding is to tell U-Net (used to generate random noise and other work) the position of reverse diffusion. Another reason for adding time embedding is that U-Net shares parameters. Adding time embedding can generate different outputs based on different inputs. Through these methods, U-Net can form some rough contours in the process of reverse diffusion. As it progresses close to the original image, we hope to obtain object edge information and some high-frequency information, so as to make the output image more realistic [25]. We utilize an attention mechanism to capture the temporal and feature dependencies of time series. To capture temporal and feature dependencies of multivariate time series, we utilize a two-dimensional attention mechanism in each residual layer instead of a convolution

architecture [26]. The attention mechanism allows the model to handle various lengths. For batch training, we apply zero padding to each sequence so that the lengths of the sequences are the same. This is also the key model used in this study.

3.3. Signal Recognition and Classification Based on DenseNet

In this section, we demonstrate the recognition and classification ability of the above comprehensive methods for Lamb wave signals of different defects in composite materials. Now we consider using neural networks for signal classification. When the network selected for signal classification is very deep, the effect of the model becomes worse (the higher the error rate), indicating that the deeper the network is, the better. When the network level increases to a certain number, the training accuracy and test accuracy are rapidly reduced, which shows that when the network becomes very deep, the deep network becomes more difficult to train. In the process of back propagation, the neural network needs to continuously propagate the gradient. When the number of network layers deepens, the gradient will gradually disappear in the process of propagation, which makes it impossible to effectively adjust the weight of the previous network layer. Therefore, deep residual network (ResNet) [27] is considered. The residual network is easier to be optimized by adding shortcut connections to "skip connections". Several layers of networks containing a shortcut connection are called a residual block, as shown in the following Figure 9:

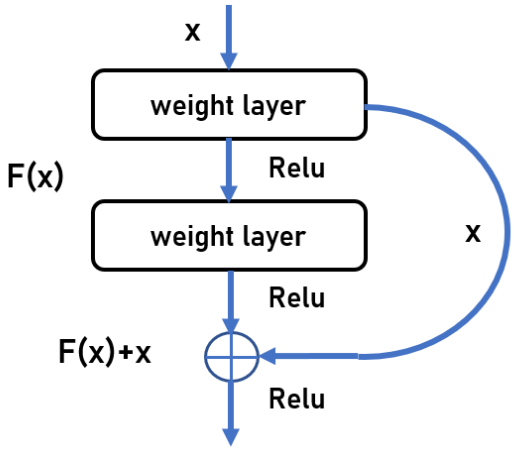

Figure 9. Schematic diagram of depth residual network.

As shown in the figure above, x represents the input, $F\ (x)$ represents the output of the residual block before the activation function of the second layer, and σ Represents the ReLU activation function. The output of the final residual block is $(F\ (x) + x)$.

Directly transfer the input x to the output as the initial result, and the output result is $H\ (x) = F\ (x) + x$. When $F(x) = 0$, then $H(x) = x$, that is, the identity mapping mentioned above. Thus, ResNet is equivalent to changing the learning goal. It is no longer a complete output of learning, but the difference between the target value $H\ (x)$ and x, that is, the so-called residual $F(x) = H\ (x) - x$. Stochastic depth shortens [28] ResNet by randomly dropping layers during training to allow better information and gradient flow.

The basic idea of the densely connected constructive network (DenseNet) model is the same as ResNet, but it establishes a dense connection between all the preceding layers and the following layers, and its name comes from this. One advantage of ResNet is that gradients can flow directly from the following layer to the front layer through the identity function. However, the output of the identity function and H is cumulative, which may hinder the information flow in the network. To improve the problem of information flow between different layers, DenseNet directly connects all inputs to the output layer. Specifically, each layer will accept all the layers in front of it as its additional input. The connection method is through element-level addition. To preserve the feed-forward nature, each layer obtains additional inputs from all preceding layers and passes

on its own feature-maps to all subsequent layers. In DenseNet, each layer is connected to the channel dimensions of all previous layers and is used as the input of the next layer. Another major feature of DenseNet is feature reuse through feature connections on the channel. These features enable DenseNet to achieve better performance than ResNet with fewer parameters and computing costs [29]. Besides better parameter efficiency, one big advantage of DenseNets is their improved flow of information and gradients throughout the network, which makes them easy to train. Each layer has direct access to the gradients from the loss function and the original input signal, leading to an implicit deep supervision.

The performance differences between the main transmission forms of these two types of networks are shown below. The nonlinear transformation equation of ResNet is as follows:

$$x_l = H_l(x_{l-1}) + x_{l-1}$$

The nonlinear transformation equation of DenseNet is as follows:

$$x_l = H_l([x_0, x_1, \ldots x_{l-1}])$$

The dense connection mode of this model has many advantages. It increases the transmission of gradient, reuses features, and even reduces overfitting on small sample data. At the same time, DenseNet has fewer parameters than ResNet, less computation and higher accuracy. The Dense block is a basic module of DenseNet, and DenseNet is divided into several Dense blocks. In each node of the Dense block, the input is concatenated feature maps, and the size of the feature maps within each Dense block is the same. A Transition module is used to perform down-sampling transition connections between each Dense block. The nonlinear combination function in the Dense block refers to the combination of BN + ReLU + Conv. The simple model structure of the Dense block is shown in Figure 10.

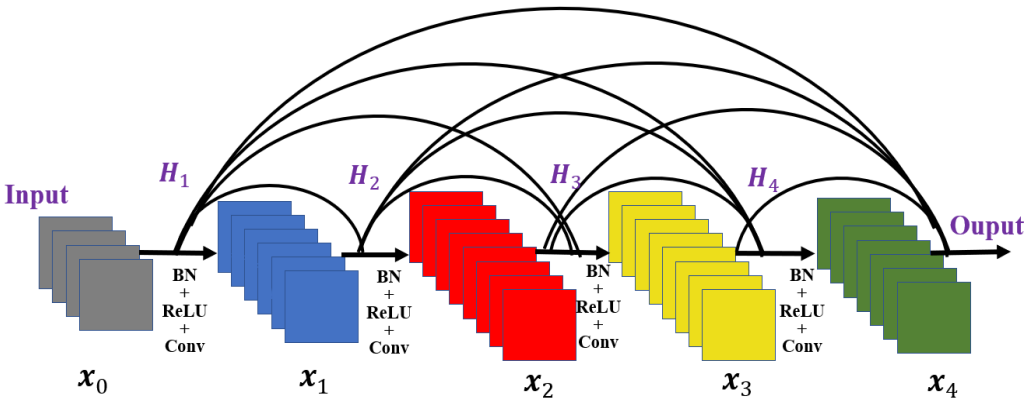

Figure 10. The simple schematic diagram of a Dense block.

Figure 11 shows a complete DenseNet structure, which includes 3 Dense Blocks and 2 Transition layers. The Transition layers connect each Dense Block and consist of convolution and pooling to downsample and compress the model. After completing these steps, the data will enter the prediction or classification module for processing. Each layer of DenseNet is designed to be very narrow to reduce redundancy. Instead of drawing representational power from extremely deep or wide architectures, DenseNet exploits the potential of the network through feature reuse, yielding condensed models that are easy to train and highly parameter-efficient. Concatenating feature-maps learned by different layers increases variation in the input of subsequent layers and improves efficiency. The network improves the flow of information and gradient, making it easy to train, and the intensive connection has regularization benefits, reducing the overfitting problem of a small training set. Additionally, after verification, the model has a good perception effect on the defect signal in this experiment and a strong feature extraction ability.

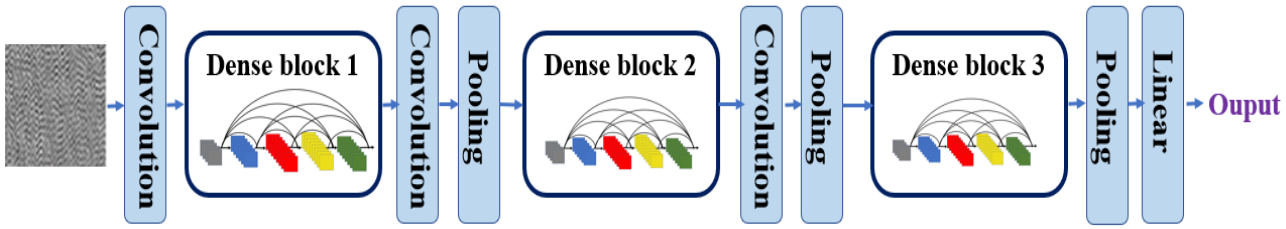

Figure 11. The overall schematic diagram of DenseNet.

4. Experimental Validation

In this section, we demonstrate the recognition and classification ability of the above comprehensive methods for Lamb wave signals of different defects in composite materials. We classify different experimental test situations, and group the existing data into corresponding training sets to train the best model.

Through the introduction and discussion in the previous chapter, it can be seen that DenseNet increases the transmission of gradients, reduces overfitting, and has low computational complexity and high accuracy. Therefore, DenseNet is used as the main model in the classification stage of the entire deep learning framework in this study. Moreover, this classifier has good perception effect on defect signals in this experiment and has strong feature extraction ability after verification. After research and optimization, the DenseNet model structure used in this experiment is shown in Table 2.

Table 2. DenseNet network structure.

Layers	Output Size	DenseNet
convolution	64 × 64	7 × 7 conv, stride2
pooling	32 × 32	3 × 3 max pool, stride2
Dense block1	32 × 32	$\begin{pmatrix} 1\times 1 \\ 3\times 3 \end{pmatrix} \times 6$
Transition layer1	32 × 32	1 × 1 conv
	16 × 16	2 × 2 average pool, stride2
Dense block2	16 × 16	$\begin{pmatrix} 1\times 1 \\ 3\times 3 \end{pmatrix} \times 12$
Transition layer2	16 × 16	1 × 1 conv
	8 × 8	2 × 2 average pool, stride2
Dense block3	8 × 8	$\begin{pmatrix} 1\times 1 \\ 3\times 3 \end{pmatrix} \times 48$
Transition layer3	8 × 8	1 × 1 conv
	4 × 4	2 × 2 average pool, stride2
Dense block4	4 × 4	$\begin{pmatrix} 1\times 1 \\ 3\times 3 \end{pmatrix} \times 32$
Classification layer	1 × 1	7 × 7 global average pool
		Fully-connected softmax

In this study, a large number of simulation data about the defect are used to test the neural network model, and the recognition ability and feature extraction ability of different neural network models for this type of defect signal are compared and ana-

lyzed, which is convenient for model selection. After converting one-dimensional data into two-dimensional images and putting them into corresponding neural networks for training, the network designed in this experiment is compared with common classification network models. This study combines the algorithms used for data expansion and classification recognition. In the data set and experimental setup, we used five combinations to test. The first is this proposed framework, which combines data augmentation and classification algorithms (including the improved DDPM). To validate the effectiveness of this method, we compared four different algorithm combinations: "VAE + DenseNet", "DCGAN + DenseNet", "DDPM + ResNet", and "DDPM + DenseNet" (including the original DDPM).

In order to test the quality and effect of data generated by different models, several common comparison indicators are selected in combination with common methods. First, the accuracy rate, that is, the ratio of the number of correctly predicted results to the total number of samples. The higher the accuracy, the better the quality of the generated data. Then there is the recall rate, which is aimed at the original sample. It means to correctly predict the probability of positive samples in all positive samples, that is, to correctly predict the ratio of the number of positive samples to all positive samples. The higher the recall rate, the more accurate results will be retrieved. Finally, Fréchet Inception Distance (FID) index is selected. FID represents the diversity and quality of generated objects. The smaller the FID, the better the diversity and quality. In the later tests, in order to highlight the overall trend and distribution characteristics, we use bold to mark the best results in different test schemes.

Next, different data grouping forms are tested to see which grouping situation has the best effect on data feature learning and recognition, and the data quality is the highest. We will adjust the number of groups and proportion relationship of three types of data, namely include intact data, hole defect data and crack defect data. The best proportion of data sets with the best learning ability for these three situations will be found by testing in different situations. The design and allocation of the experiment are shown in Table 3, the best values in each test result are marked in bold:

Table 3. Different data grouping forms and test results.

Intact Data Volume	Hole Data Volume	Crack Data Volume	FID	Recall	Accuracy
20	80	80	26.23	0.51	78.16
40	80	80	38.04	0.62	84.00
80	80	80	18.15	**0.78**	87.15
160	80	80	**12.37**	0.72	**88.37**
320	80	80	16.35	0.31	87.42

Through the table, we can observe that the fourth group should be selected for experiment and training. In this grouping case, the lowest FID value and the highest accuracy rate can be obtained, and the higher recall value can also be maintained, indicating that the learning and training effect of input data is the best in this case.

After determining the classification method of data groups, use the classification method with the best learning effect mentioned above, and use the data collected from the experiment to make a training set. First, the generation model is used to expand the unbalanced data of some samples, and then the expanded data is mixed with the original data to make a new dataset. Then put, the new data set obtained after learning and training into the previously selected classification network for testing, and verify the overall experimental design through the accuracy and effect of classification. Relevant details of the training process are supplemented as follows. For the dataset, we randomly divided the dataset into five parts and used one of them as test data for each run. We also randomly split the remaining data into train and validation data with a ratio of 6:1. For the training of

all tasks, we normalize each feature to have zero mean and unit variance. We set the batch size as 16 and the number of epochs as 200. We used Adam optimizer with a learning rate of 0.001. The core values in the diffusion model are also given here. We set the number of the diffusion step T = 100, the minimum noise level β_1 = 0.0001, and the maximum noise level β_T = 0.5. For the several types of data enhancement and data classification methods used in this study, grouping and collocation tests are conducted, respectively. This is to test which data enhancement and data classification methods work best.

After determining the testing plan and training details, extensive training and testing were conducted for the five methods proposed earlier in this experiment. The framework combining data augmentation and classification algorithms (including the improved DDPM) proposed in this paper, as well as four different algorithm combinations: "VAE + DenseNet", "DCGAN + DenseNet", "DDPM + ResNet", and "DDPM + DenseNet" (including the original DDPM), were tested as a whole. In addition to the accuracy index, the FID index was also retained as a reference in the final test results. After multiple rounds of training, the results are shown in Table 4 and the best values in each test result are marked in bold:

Table 4. Test results of different combinations of data enhancement and data classification methods.

Models Used	FID	Accuracy
VAE + DenseNet	41.65	71.25
DCGAN + DenseNet	33.56	86.17
DDPM + ResNet	28.33	85.42
DDPM + DenseNet	25.10	86.37
Proposed framework	**13.74**	**88.10**

It can be seen that the improved DDPM model is the best for learning and generating such defect signals. The accuracy obtained by putting the generated data back into the classification model is also the highest, and the performance is relatively stable. Hence, suggesting that this type of architecture is well suited to detect features and patterns in the raw time-domain signals that can unequivocally determine the presence of defect reflections. For the signal data of this experiment, DDPM can extract features well, and generate new signals that are close to the original signal properties, which plays a great role in defect signal processing and recognition. At the same time, we evaluated the effect of DenseNet in the classification task and compared it with ResNet architecture. The feature extraction ability and classification effect of Densenet in this study are also stronger than Resnet, and these two methods can be better complementary and improved. To sum up, the signal recognition neural network framework proposed in this experiment combined with improved DDPM and DenseNet shows good comprehensive effect in the above tests.

The experiment and test results show that the method designed in this study based on DenseNet classification and DDPM data enhancement can accurately detect and classify the damage signals of common defects in CFRP composite plates, and can achieve high accuracy. It is practical for the nondestructive testing of composite materials.

5. Conclusions

In this study, a method for identifying and classifying composite damage signals based on DenseNet classification and DDPM data enhancement is proposed. At the same time, a dimension transformation method is introduced to process defect signals. This method converts one-dimensional timing signals into two-dimensional images, which is convenient for combining the data with the latest and most mature neural network system. This method, by adding attention mechanism and other related parameter designs, has been successfully improved. After determining the test plan and training details, the five application methods proposed at the end of this experiment were fully trained and tested, and the advantages and disadvantages of the proposed method and the other combination methods were compared. The experiment and test results show that the method designed

in this study based on DenseNet classification and DDPM data enhancement can accurately detect and classify the damage signals of common defects in CFRP composite plates, and can achieve high accuracy. In the final comprehensive test, the test results of the method proposed in this study for Lamb wave signal-datasets of different defects reached 88.10%. Compared with other common data expansion and signal classification methods, this scheme also has advantages, and is practical for the nondestructive testing of composite materials. The method proposed in this experiment mainly focuses on the study of micro-damage in composite structures, and it may not be able to detect defects smaller than 1 mm. The application object of this method is mainly carbon fiber composites, but it can also be applied to other composite materials, such as glass fiber, and has been tested, whereas other materials have not been tested yet. In the future, we may try to extend it to other materials and other types of damage, and further improve the accuracy. We believe that this scheme will continue to improve accuracy in the future and will be extended to more types and components of composite products; it may play a role in composite nondestructive testing and structural health monitoring.

Author Contributions: Validation, Z.L.; Investigation, Y.H.; Writing-original draft, T.H.; Writing-review & editing, Y.H.; Supervision, Y.G. and F.X.; Funding acquisition, Y.G. All authors have read and agreed to the published version of the manuscript.

Funding: This project was supported by the National Natural Science Foundation of China (Grant Nos. 52275146, 51835003, 61804054 and 12174102), supported by State Key Laboratory of New Textile Materials and Advanced Processing Technologies No. XXXFZ2022006, and supported by "the Fundamental Research Funds for the Central Universities".

Institutional Review Board Statement: Not applicable.

Informed Consent Statement: Not applicable.

Data Availability Statement: Not applicable.

Conflicts of Interest: The authors declare no conflict of interest.

References

1. Gibson, F.R. A review of recent research on mechanics of multifunctional composite materials and structures. *Compos. Struct.* **2010**, *92*, 2793–2810. [CrossRef]
2. Gomes, G.F.; Mendéz, Y.A.D.; Alexandrino, P.D.S.L.; da Cunha, S.S., Jr.; Ancelotti, A.C., Jr. The use of intelligent computational tools for damage detection and identification with an emphasis on composites—A review. *Compos. Struct.* **2018**, *196*, 44–54. [CrossRef]
3. Xu, Y.; Wen, W.-D.; Cui, H.-T. Progressive fatigue damage analysis method of laminated composites. *J. Aerosp. Power* **2007**, *22*, 602–607.
4. Qing, X.L.; Li, W.Z.; Wang, Y.S.; Sun, H. Piezoelectric Transducer-Based Structural Health Monitoring for Aircraft Applications. *Sensors* **2019**, *19*, 545. [CrossRef]
5. Xu, C.B.; Yang, Z.B.; Tian, S.H.; Chen, X.F. Lamb wave inspection for composite laminates using a combined method of sparse reconstruction and delay-and-sum. *Compos. Struct.* **2019**, *223*, 110973. [CrossRef]
6. Xu, C.B.; Yang, Z.B.; Qiao, B.J.; Chen, X.F. Traveling distance estimation for dispersive Lamb waves through sparse Bayesian learning strategy. *Smart Mater. Struct.* **2019**, *28*, 085008. [CrossRef]
7. Jhang, K.Y. Nonlinear Ultrasonic Techniques for Nondestructive Assessment of Micro Damage in Material: A Review. *Int. J. Precis. Eng. Manuf.* **2009**, *11*, 123–135. [CrossRef]
8. Mirahmadi, S.J.; Honarvar, F. Application of signal processing techniques to ultrasonic testing of plates by S_0 Lamb wave mode. *NDT E Int.* **2011**, *44*, 131–137. [CrossRef]
9. Xu, J.C.; Zhu, W.J.; Xiang, Y.X.; Gao, Y.; Qiu, X. Localization and Imaging of Micro-Cracks Using Nonlinear Lamb Waves with Imperfect Group-Velocity Matching. *Appl. Sci.* **2021**, *11*, 8069. [CrossRef]
10. Gandomi, A.; Haider, M. Beyond the hype: Big data concepts, methods, and analytics. *Int. J. Inf. Manag.* **2015**, *35*, 137–144. [CrossRef]
11. Schmidhuber, J. Deep Learning in Neural Networks: An Overview. *Neural Netw.* **2015**, *61*, 85–117. [CrossRef]
12. Lu, C.; Wang, Y.; Ragulskis, M.; Cheng, Y. Fault Diagnosis for Rotating Machinery: A Method based on Image Processing. *PLoS ONE* **2016**, *11*, e0164111. [CrossRef]
13. Ince, T.; Kiranyaz, S.; Eren, L.; Askar, M.; Gabbouj, M. Real-time motor fault detection by 1D convolutional neural networks. *IEEE Trans. Ind. Electron.* **2016**, *63*, 7067–7075. [CrossRef]

14. Abdeljaber, O.; Avci, O.; Kiranyaz, S.; Gabbouj, M.; Inman, D.J. Real-time vibration-based structural damage detection using one-dimensional convolutional neural networks. *J. Sound Vib.* **2017**, *388*, 154–170. [CrossRef]
15. Do, V.T.; Chong, U.P. Signal Model-Based Fault Detection and Diagnosis for Induction Motors Using Features of Vibration Signal in Two-Dimension Domain. *Stroj. Vestn.* **2011**, *57*, 655–666. [CrossRef]
16. Liu, H.; Zhang, Y. Deep learning based crack damage detection technique for thin plate structures using guided lamb wave signals. *Smart Mater. Struct.* **2020**, *29*, 015032. [CrossRef]
17. Wu, J.; Xu, X.; Liu, C.; Deng, C.; Shao, X. Lamb wave-based damage detection of composite structures using deep convolutional neural network and continuous wavelet transform. *Compos. Struct.* **2021**, *276*, 114590. [CrossRef]
18. Wen, L.; Li, X.; Gao, L.; Zhang, Y. A New Convolutional Neural Network Based Data-Driven Fault Diagnosis Method. *IEEE Trans. Ind. Electron.* **2018**, *65*, 5990–5998. [CrossRef]
19. Foomani, G.H.; Anisuzzaman, D.M.; Niezgoda, J.; Niezgoda, J.; Guns, W.; Gopalakrishnan, S.; Yu, Z.-Y. Synthesizing time-series wound prognosis factors from electronic medical records using generative adversarial networks. *J. Biomed. Inform.* **2021**, *125*, 103972. [CrossRef]
20. Sohl-Dickstein, J.; Weiss, E.; Maheswaranathan, N.; Ganguli, S. Deep Unsupervised Learning using Nonequilibrium Thermodynamics. In Proceedings of the 32nd International Conference on Machine Learning (ICML), Lille, France, 6–11 July 2015.
21. Ruttor, A.; Batz, P.; Opper, M. Approximate Gaussian process inference for the drift function in stochastic differential equations. In Proceedings of the 26th International Conference on Neural Information Processing Systems, Lake Tahoe, NV, USA, 5–10 December 2013; pp. 2040–2048.
22. Song, Y.; Sohl-Dickstein, J.; Kingma, D.P.; Kumar, A.; Ermon, S.; Poole, B. Score-based generative modeling through stochastic differential equations. *arXiv* **2020**, arXiv:2011.13456.
23. Ho, J.; Jain, A.; Abbeel, P. Denoising diffusion probabilistic models. *Adv. Neural Inf. Process. Syst.* **2020**, *33*, 6840–6851.
24. Song, Y.; Ermon, S. Generative modeling by estimating gradients of the data distribution. In *Advances in Neural Information Processing Systems 32*; Curran Associates Inc.: Red Hook, NY, USA, 2019; pp. 11895–11907.
25. Song, Y.; Kingma, P.D. How to train your energy-based models. *arXiv* **2021**, arXiv:2101.03288.
26. Narayan, S.S.; Marlin, B.M. Multi-Time Attention Networks for Irregularly Sampled Time Series. In Proceedings of the ICLR 2021, Virtual, 3–7 May 2021; Available online: https://iclr.cc/Conferences/2021 (accessed on 30 January 2021).
27. He, K.; Zhang, X.; Ren, S.; Sun, J. Deep residual learning for image recognition. In Proceedings of the IEEE Conference on Computer Vision and Pattern Recognition, Las Vegas, NV, USA, 27–30 June 2016; pp. 770–778.
28. Huang, G.; Sun, Y.; Liu, Z.; Sedra, D.; Weinberger, K. Deep Networks with Stochastic Depth. In Proceedings of the 14th European Conference, Amsterdam, The Netherlands, 11–14 October 2016.
29. Huang, G.; Liu, Z.; Van Der Maaten, L.; Weinberger, K.Q. Densely connected convolutional networks. In Proceedings of the IEEE Conference on Computer Vision and Pattern Recognition, Long Beach, CA, USA, 21–26 July 2017; pp. 4700–4708.